



**ADVANCES IN
FOREST FIRE
RESEARCH**

DOMINGOS XAVIER VIEGAS

EDITOR

2014

Wind flow characterization associated with fire behaviour measurements

Dan Jimenez^a, Bret W. Butler^a, Casey Teske^b, Joseph O'Brien^c, Louise Loudermilk^c, Ben Hornsby^c, Craig Clements^d

^a USDA Forest Service, Rocky Mountain Research Station 5775 W US Highway 10 Missoula MT 59808, USA

^b National Center for Landscape Fire Analysis, University of Montana, Missoula, MT 59812, USA

^c USDA Forest Service, Southern Research Station, 200 W.T. Weaver Blvd. Asheville, NC 28804, USA

^d Fire Weather Research Laboratory, Department of Meteorology and Climate Science, San Jose State University San Jose, CA USA

Abstract

The relationship between fire behaviour and ambient wind flow is often presumed, but seldom measured. General understanding of observed fire behaviour suggests an increase in fire intensity associated with increased wind speed (Van Wagner 1987, Rothermel 1991, Finny *et al.* 2006, Forthofer 2007). Fire behaviour characteristics (such as temperature, radiant and total heat flux, 2- and 3-dimensional velocities, and air flow) are extremely difficult to measure in-situ (Jimenez *et al.* 2007). Studies base on these phenomena often correlate empirical data either from observed wildland fire or laboratory experiments, but few data sets exist that capture ambient wind flow simultaneously with corresponding in-situ fire behaviour measurements.

This paper reports on the corresponding fire behaviour and wind field relationship on six field study plots that were instrumented with several fire behaviour packages (Butler *et al.* 2004), and a network of wind anemometer towers deployed around the perimeter of each plot. The study plots were part of the Prescribed Fire Combustion and Atmospheric Dynamics Research Experiment (RxCADRE) 2012 field campaign, with the objectives aimed at developing synergies between fuels, fuel consumption, fire behaviour, smoke management, and fire effects measurements for fire model development and evaluation.

Keywords: *Fire behaviour, prescribed fire, surface wind flow, anemometer, thermography*

1. Introduction

Fire-atmosphere interactions (FAI) are defined as the interactions between presently burning fuels and the atmosphere, in addition to interactions between fuels that will eventually burn in a given fire and the atmosphere (Potter 2012). Currently, much of the meteorological sampling for fire behaviour applications and science is performed at a very coarse resolution (i.e., hundreds of meters to kilometers), such as the standard Remote Automated Weather Stations (RAWS) networks in existence throughout the United States (Horel and Dong 2010). Additionally, these data are often captured or averaged at a coarse time resolution (i.e., hourly to daily), although surface flows are constantly fluctuating.

Wildland fire researchers have recognized the benefit of in-situ measurements of fire intensity and behaviour as a critical component in the effort to develop improved fire management decision support models. Past measurements consisted primarily of observations of rate of spread, gas temperatures, and fuel consumption, and have been both field based (Barrows 1951; Cheney *et al.* 1993; Fons 1946) and laboratory based (Catchpole *et al.* 1998; Fons 1946; Rothermel 1972). New mathematical models include additional physics which has led to the need for additional measurements, particularly of the basic heat and chemical processes occurring in fire in addition to the local surface wind flow.

Recent studies have focused on understanding the role of both radiative and convective energy transport to wildland fire ignition and spread (Morandini and Silvani 2010).

When considering relationships between energy transport in wildland flames and particle ignition it is unclear how small particles respond to temporal fluctuations in the heating source. Thus the temporal characteristics of the heating regime are relevant to increased understanding of wildland fire behaviour (Frankman *et al.* 2012)

There is an increasing need to measure fire-atmosphere interactions at finer scales in order to better understand the role of near-surface wind and thermodynamic structures of fire behaviour (Clements *et al.* 2007). While useful at a landscape scale and possibly for the largest fires, both spatial and temporal scales of near-surface wind and thermodynamic structures presently are highly generalized. Interpolation between these sparsely dispersed points does not consider the spatial heterogeneity or micro-scale influences that impact the smaller fires on the landscape, nor do they capture the fluctuations at a fine temporal scale.

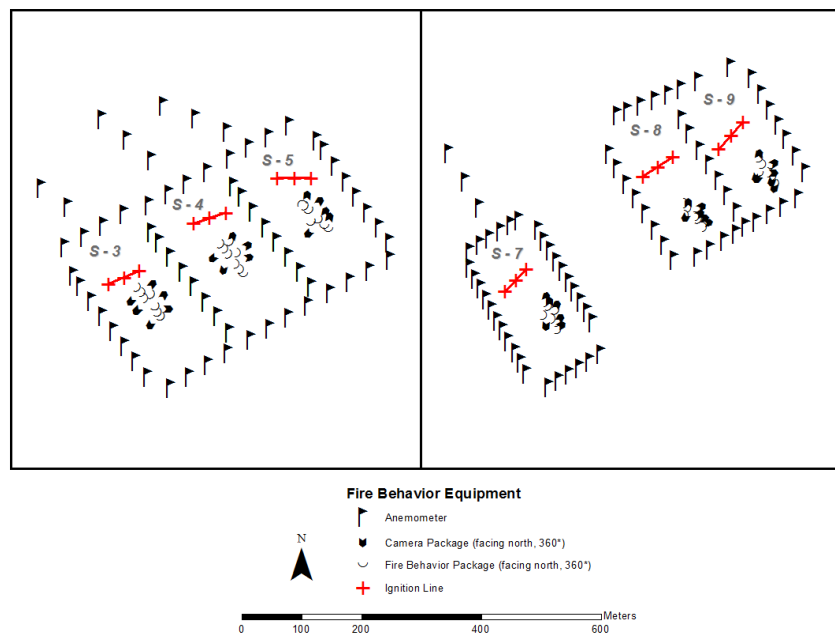


Figure 1. Equipment layout for the six 100mx200m plots.

For this study, six plots (S3, S4, S5, S7, S8, S9) measuring roughly 100m x 200m, and oriented in a northwest/southeast (long-axis) alignment, were highly instrumented in order to capture time-resolved surface wind flow and corresponding in-situ fire behaviour (Figure 1). The plots were chosen and aligned based on generally homogenous fuels and predicted general wind direction. Plots S3, 4, and 5 were in a predominantly grass fuel type, while plots S7, 8, and 9 were in a predominantly grass/shrub fuel type. Multiple cup-and-vane anemometers were set up with 20m spacing around each plot, with adjacent plot edges sharing anemometers. Additionally, five to seven in-situ fire behaviour packages (FBPs) recording heat flux, air temperature, and 2-D mass flow at 10Hz were deployed within each of the plots in order to characterize the fire behaviour throughout plot ignition. Finally, visible and infrared 1Hz-averaged imagery were collected from an elevated 26m platform located at the upwind edge of each plot. All instruments were synchronized to Greenwich Mean Time (GMT).

2. Methods – Surface Wind Field Measurements

The six replicate burn blocks were burned during two separate burning periods. Three of the replicates (S3, S4, S5) were individually burned on November 1, 2012; the other three replicates (S7, S8, S9) were individually burned on November 7, 2012. In order to provide a continuous flaming front, two

lighters with drip torches uniformly and rapidly ignited the burn blocks, starting at the middle point of the ignition line and simultaneously working in opposite directions toward both ends; these points are marked in Figure 1. Detailed fuels, fuel consumption, fire behaviour, heat flux, and fire effects data were collected on the plots before and during the burns. Table 1 provides instrumentation and ignition specifics for each replicate burn block.

Surface wind and surface fire behaviour measurements were collected on all burn units. Multiple cup-and-vane anemometers (S-WCA-M003, Onset Computer Corporation) were set up with approximately 20m spacing around each small plot, with adjacent plot edges sharing anemometers (Figure 1; Table 1). These instruments measure wind speed and direction at 3.3m above ground level (AGL); the data are used to characterize surface flow patterns before and during the burns. Cup revolutions and unit vector components are accumulated every three seconds for the duration of the logging interval. Wind speed is the average speed for the entire logging interval ($0-44 \text{ m/s} \pm 0-4\%$). Gust speed is the highest three-second wind recorded during the logging interval. Average direction is calculated from the average of the vector components ($0-358^\circ \pm 5^\circ$).

Table 1. Burn plot instrumentation and ignition information.

Burn Unit	Burn Date	Burn Start Time (Zulu)	Data		Plot Instrumentation
			Collection	End Time (Zulu)	
S3	11/1/2012	21:20	22:30		Anemometer: 24 adjacent to plot; 2 NW of plot FBPs: 7; Cameras: 6
S4	11/1/2012	19:35	21:15		Anemometer: 24 adjacent to plot; 3 NW of plot FBPs: 8; Cameras: 5
S5	11/1/2012	18:10	19:30		Anemometer: 24 adjacent to plot; 3 NW of plot FBPs: 7; Cameras: 5
S7	11/7/2012	17:25	18:50		Anemometer: 33 adjacent to plot; 3 NW of plot FBPs: 7; Cameras: 6
S8	11/7/2012	20:16	21:30		Anemometer: 25 adjacent to plot FBPs: 6; Cameras: 6
S9	11/7/2012	18:54	20:10		Anemometer: 23 adjacent to plot FBPs: 7; Cameras: 7

2.1. Methods – In-Situ Energy Measurements

In-situ fire behaviour was measured using portable fire behaviour packages (FBPs) developed at the US Forest Service, RMRS Fire Science Lab. The FBPs measure air temperature during fire passage, radiant and convective heat flux emitted from the flames and horizontal and vertical air flow. The sensor package measures 27 cm by 15 cm by 18 cm and in its current configuration weighs approximately 5.3 kg. Various enclosure materials consist of 0.37mm thick aluminium welded at the seams. A 12 volt 4.5 Ah sealed lithium polymer battery provides power to the sensor array and data logger. The data loggers used are Campbell Scientific® model CR1000 and are capable of logging over one million samples, providing 3.5 hours of continuous data logging at 10 Hz. This logger is user-programmable and accepts a wide range of analog and digital inputs and outputs. All of the FBPs incorporate a Medtherm® Dual Sensor Heat Flux sensor (Model 64-20T) that provide incident total and radiant energy flux, a type K fine wire thermocouple (nominally 0.05 mm diameter wire) for measuring gas temperature, a custom designed narrow angle radiometer (Butler 1993) to characterize flame emissive power, and two pressure based flow sensors (McCaffrey and Heskestad 1976) to characterize air flow. Table 2 provides details about individual sensors and their engineering specifications.

Table 2. In-situ Fire Behaviour Package (FBP) Specifications

Narrow Angle	
Sensor	20-40 element thermopile
Spectral Band of Sensor	0.15 – 7.0 μm with sapphire window
Field of View	$\sim 4.5^\circ$ controlled by aperture in sensor housing
Transient Response	Time constant of sensor nominally 30msec
Units of Measurement	Calibrated to provide emissive power of volume in FOV in kW/m^2
Total Energy Sensor	Medtherm Corp® Model 64-20T Dual total Heat Flux Sensor/Radiometer
Sensor	Schmidt-Boelter Thermopile
Spectral Band of Sensor	All incident thermal energy
Field of View	$\sim 130^\circ$ controlled by aperture in sensor housing
Transient Response	< 290msec
Units of Measurement	Total heat flux incident on sensor face in kW/m^2
Hemispherical Radiometer	Medtherm Corp® Model 64-20T Dual total Heat Flux Sensor/Radiometer
Sensor	Schmidt-Boelter Thermopile (Medtherm Inc)
Spectral Band of Sensor	0.15 – 7.0 μm with sapphire window
Field of View	$\sim 130^\circ$ controlled by window aperture
Transient Response	< 290msec
Units of Measurement	Radiant energy incident on sensor face in kW/m^2
Air Temperature	
Sensor	Type K bare wire butt welded thermocouple, new, shiny, connected to 27ga lead wire
Wire Diameter	0.05mm
Bead Diameter	$\sim 0.08\text{-}0.13\text{mm}$
Units of Measurement	Degrees Celsius
Air Mass Flow	
Sensor	SDXL005D4 temperature compensated differential pressure sensor
Pressure Range	0-5 in H_2O
Sensor Design	Pressure sensor is coupled to custom designed bidirectional probe with $\pm 60^\circ$ directional sensitivity.
Units of Measurement	Calibrated to convert dynamic pressure to velocity in m-s^{-1} assuming incompressible flow
Sensor Housing	150 \times 180 \times 270 (mm)
Housing Weight	7.7 kg
Insulation Material	Cotronics Corp® 2.5cm thick ceramic blanket
Tripod Mount	$\frac{1}{2}$ inch female NCT fitting permanently mounted to base of enclosure.
Power Requirements	12V DC
Power Supply	Rechargeable Internal Battery
Data Logging	Campbell Scientific Model CR1000
Sampling Frequency	Variable but generally set at 10 Hz

The sensors were calibrated prior to deployment as described elsewhere (Butler and Jimenez 2009). Integration of the heat flux time histories can provide a measure of fire total, radiative and convective energy per unit area as a function of heating time. In all cases the FBPs were positioned to sense fire from the expected spread direction (e.g., facing the oncoming fire front) based on wind direction, terrain, and lighting procedures. All FBPs were located nominally 1.0 m above the mineral soil. Incident radiant and total heat flux at the surface of the FBPs were evaluated to determine convective heating at the sensor face (Frankman *et al.* 2010). The fine wire thermocouple has a response time of approximately 0.01 s and was used to sense flame presence and flame residence time. Flame arrival at the FBP was indicated by a nearly vertical increase ($\sim 3000\text{-}5000^\circ\text{C/s}$) in temperature to several hundreds of degrees above ambient. This temperature increase was almost always associated with a nearly instantaneous increase in heat flux at the sensor ($4\text{ to }25\text{ kW/m}^2/\text{s}$). The completion of the flame event was indicated by a rapid decay in air temperature. In some cases the thermocouple failed, in which case the radiometer data alone was used to gauge the arrival and completion of flaming combustion. Flame radiative and convective energy were calculated by integrating the respective signals over the period of flaming combustion.

2.2. Methods – Infrared Thermography Measurements

Visible and near infrared (IR) imagery were captured using cameras situated on a 26 m boom lift. To lessen the likelihood of unburned fuels obscuring the IR signal from the fire, the lift was located 10-25 m from the control lines demarcating the small units; it was positioned at the centre of and perpendicular to the ignition line upwind of the units in all cases except S9. Prior to ignition of each plot, an image of the plot indicating the ambient temperature range ($0\text{-}300\text{ C}$) was collected. The oblique IR imagery was collected using a FLIR Inc SC660. The SC660 has a focal plane array resolution of 640×480 pixels, a sensitivity of 0.03°C , spatial resolution of 1.3 mrad and a thermal accuracy of $\pm 2\%$. The field of view of the oblique imagery covered the majority of the area of the small burn blocks and captured the entire fire perimeter from ignition until the fire passed the central instrument cluster and/or reached the downwind control line. Emissivity was set at 0.98 and the air temperature and relative humidity were noted for post processing. The temperature range for all cameras during the fires was set to $300\text{-}1500^\circ\text{C}$ for collecting active fire IR data. High definition digital visual imagery was collected before and during the fire from video cameras located adjacent to the IR cameras. Post-processing resolution of this imagery is $1\text{ m} \times 1\text{ m}$.

Twelve ground control points for each small burn block were identified using surveyed positions of hot targets, instruments, and ignition points. The pre-fire IR image was critical for identifying ground control points.

For all IR imagery, the native file format was converted to an ASCII array of temperatures in K with rows and three columns where $x,y,z = \text{pixel row, pixel column, and temperature}$. Temperatures were then converted into W m^{-2} using the Stefan-Boltzmann equation for a gray body emitter. Mean residence time was calculated as the average amount of time a pixel was measured to be $>525^\circ\text{C}$ (Draper point) and maximum residence time was the maximum number of times a single pixel was measured to be $>525^\circ\text{C}$.

For the oblique platform, images were processed using Python 2.7 programming language and rectified using GDAL (Geospatial Data Abstraction Library, 1.10.1, www.gdal.org). Once rectified, each image was converted back to radiometric temperature values, by back calculating using the previous equations, and estimates of fire radiative power (FRP) by pixel were calculated using the Stefan-Boltzmann Law for a grey body emitter.

Fire pixel values were summed across units at each time step to give total fire radiative energy (FRE) for the whole fire. Total fire radiative energy density (FRED) was calculated across oblique IR images (Figure 2). The total FRED images visually illustrate the area recorded by the oblique IR camera, as well as the distortion caused by the oblique angle.

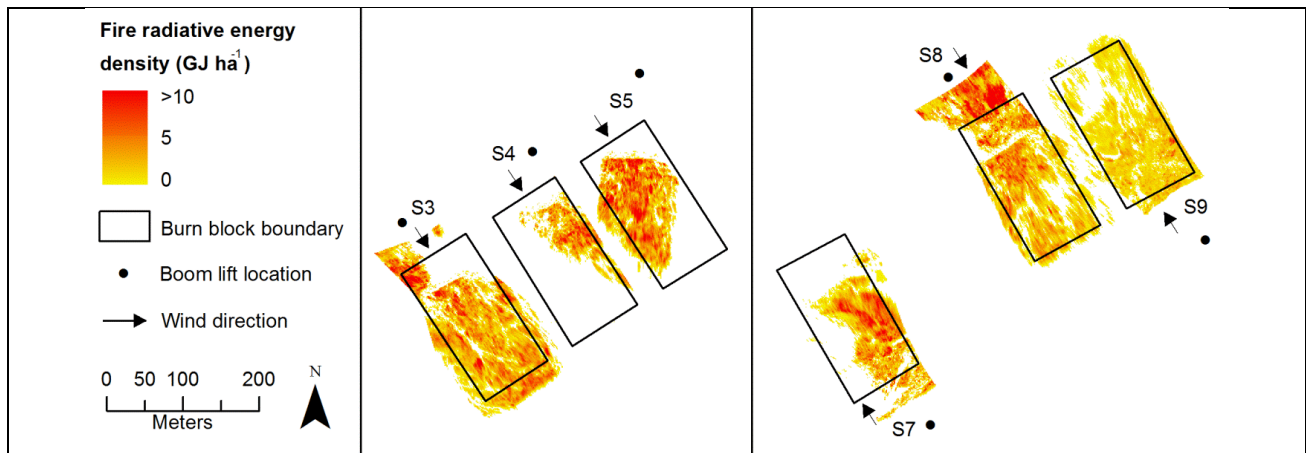


Figure 2. Total FRED ($GJ ha^{-1}$) across oblique IR imagery.

3. Results and Discussion

The aim of the RxCADRE campaign effort was to simultaneously acquire fine- to coarse-scale fuels, weather, and fire behaviour information during a suite of low-intensity prescribed fire experiments. This paper outlines a dense instrumentation network designed to measure the fine-scale meteorology within and around each burn block and couple that with fire behaviour and effects.

Preliminary results suggest that multiple fire behaviour and fire weather platforms can successfully capture small scale fire and terrain induced fluctuations, which may influence local fire-atmosphere interactions at the fire front. Initial analyses of the cup-and-vane anemometer data suggest that the relatively low fire intensity may not have been powerful enough to influence local weather conditions, as wind speed and direction differences related to the passage of the fire front were not detectable within the gridded surface level anemometer array. Table 3 outlines the overall average wind direction and speed, as well as the minimum and maximum wind speed, measured during each burning period for each of the six plots.

Table 3. Overall measurements for the cup-and-vane anemometer

Plot	Average Wind Direction, ϕ	Average Wind Speed, mph	Minimum Wind Speed, mph	Maximum Wind Speed, mph
S3	275.66	5.29	0.00	14.94
S4	275.06	7.65	0.00	18.03
S5	251.12	6.51	0.00	16.20
S7	274.69	8.08	0.00	19.15
S8	292.35	9.01	0.00	21.97
S9	270.30	9.03	0.00	21.59

For this study fire intensity was measured both in-situ by FBPs and remotely from IR cameras on an elevated oblique angle platform. The fire behaviour per unit (e.g., each of the six plots) is further interpreted using visual observations of flame properties; derived rate of spread values (based on observations of visual video footage, calculations based on infrared images, and fire time of arrival at fire behaviour packages); air temperature measurements; total and radiant energy measured incident on the in-situ FBPs; and derived values for fire radiative energy and fire convective energy.

Table 4 presents measurements derived from the FBP data for each of the six replicate burn blocks. These measurements include average radiative heat flux over the flaming period (Q_R), average convective flux over the flaming period (Q_C), average total heat flux at sensor for the flaming period

(Q_T), averaged flame emissive power from the narrow angle sensor (E_F), averaged kinetic air temperature (T_{air}) and averaged flame residence time from heat flux data (t_{flame}) for each of the burn plots. In general, the shrub/grass plots (S7,8,9) showed higher radiant, convective, and total heat flux, as well as higher emissive power than the grass plots (S3,4,5).

Table 5 outlines measurements derived from the oblique IR imagery for each of the six plots. Measurements include the active flaming duration, mean active flaming area, total area burned, total FRE, Mean FRP, Max FRP, and mean FRED. Total area burned is the mean number of $1m^2$ pixels burned at 1Hz (across IR images), and excludes unburned areas (pixels) within burn blocks.

Table 4. Averaged in-situ fire behaviour package data for each plot.

Plot	Average Radiant Heat Flux (kW/m^2)	Average Convective Heat Flux (kW/m^2)	Average Total Heat Flux (kW/m^2)	Average Flame Emissive Power (kW/m^2)	Average Kinetic Air Temperature (C)	Average Flame Residence Time (sec)
S3	7.5	5.9	12.1	23.0	821.6	103
S4	3.6	1.2	4.5	15.1	463	211
S5	3.7	5.5	8.6	14.5	682	12.3
S7	10.5	10.2	19.9	44.1	707	204
S8	12.9	12.5	23.7	42.8	922	122
S9	11.7	8.9	19.4	30.3	780.6	93

Table 5: Oblique IR imagery data for each plot.

Plot	Active flaming duration (min)	Mean (SD) active flaming area (m^2)	Total area burned (ha)	Total FRE (GJ)	Mean (SD) FRP (MW)	Max FRP (MW)	Mean (SD) FRED ($GJ ha^{-1}$)
S3	26	324 (286)	2.16	5.7	4.2 (3.8)	15.4	3.0 (2.5)
S4	20	88 (86)	0.50	1.3	1.2 (1.4)	5.5	3.0 (2.5)
S5	29	289 (203)	1.14	5.9	3.9 (3.0)	14.0	3.9 (2.9)
S7	29	150 (217)	1.14	3.1	2.1(3.3)	18.8	3.0 (2.6)
S8	23	353 (356)	2.31	6.3	5.1 (6.7)	41.4	3.0 (3.1)
S9	17	177 (173)	1.82	1.9	2.0 (2.0)	7.8	1.2 (1.0)

Comparisons between the in-situ fire behaviour measurements and oblique IR are not complete and therefore are not presented in this paper. However; the in-situ point source data show slightly greater heat flux measurements in plots S7-S9 which is in alignment with the grass/shrub fuel complex versus the dominant grass fuel component in plots S3-S5. A similar trend is not as apparent in the oblique IR data.

The calculations and analysis used between point source measurements (FBPs) and landscape scale measurements (IR) show promising similarities and it is our belief that the two techniques provide in depth detail pertaining to the micro scale fire environment. In these six low intensity grass fires, the interactions between fire behaviour and ambient wind flow are non-existent or difficult to detect. However, similar replicated measurements in a high intensity shrub or forest fire might elucidate some relationship between fire behaviour and micrometeorology. From this study we hope to determine that precise measurements at multiple scales in space and time are important for capturing and understanding the variability associated with both large and small scale fires in terms of wind flow and fire behaviour.

4. References

- Barrows JS (1951) 'Fire behaviour in northern Rocky Mountain forests. USDA Forest Service, Station Paper No. 29. (Missoula, MT)
- Butler, BW (1993) Experimental measurements of radiant heat fluxes from simulated wildfire flames. In '12th International Conference of Fire and Forest Meteorology, Oct. 26-28, 1993. Jekyll Island, Georgia', Oct. 26-28, 1993. (Eds JM Saveland, J Cohen) Volume 1 pp. 104-111. (Society of American Foresters, Bethesda, MD:
- Butler, BW, Jimenez, D (2009) In situ measurements of fire behavior. In '4th International Fire Ecology & Management Congress: Fire as a Global Process. Savannah, GA', 30 November - 4 December, 2009. (Ed. S Rideout-Hanzak) (The Association for Fire Ecology:
- Butler, BW, Cohen, J, Latham, DJ, Schuette, RD, Sopko, P, Shannon, KS, Jimenez, D, Bradshaw, LS (2004) Measurements of radiant emissive power and temperatures in crown fires. *Canadian Journal of Forest Research* 34, 1577- 1587.
- Catchpole WR, Catchpole EA, Butler BW, Rothermel RC, Morris GA, Latham DJ (1998) Rate of spread of free-burning fires in woody fuels in a wind tunnel. *Combustion Science Technology* 131, 1-37.
- Cheney NP, Gould JS, Catchpole WR (1993) The influence of fuel, weather and fire shape variables on fire-spread in grasslands. *International Journal of Wildland Fire* 3, 31-44.
- Clements, C. B., S. Zhong, S. Goodrick, J. Li, X. Bian, B.E. Potter, W. E. Heilman, J.J. Charney, R. Perna, M. Jang, D. Lee, M.Patel,S. Street and G. Aumann 2007: Observing the Dynamics of Wildland Grass Fires: FireFlux- A Field Validation Experiment. *Bull. Amer. Meteor. Soc.*, 88(9), 1369-1382.
- Finney, M.A., R.C. Seli, C.W. McHugh, A.A. Ager, B. Bahro, J.K. Agee. 2006. Simulation of long-term landscape-level fuel treatment effects on large wildfires. *USDA Forest Service Proceedings RMRS-P-41*.
- Fons WL (1946) Analysis of fire spread in light forest fuels. *Journal of Agricultural Engineering Research* 72, 93-121.
- Forthofer, J. M. 2007. Modeling wind in complex terrain for use in fire spread prediction. Fort Collins, CO: Colorado State University, Thesis. (528 KB, 123 pages).
- Frankman, D, Webb, BW, Butler, BW, Jimenez, D, Forthofer, JM, Sopko, P, Shannon, KS, Hiers, JK, Ottmar, RD (2012) Measurements of convective and radiative heating in wildland fires. *International Journal of Wildland Fire* 22, 157-167.
- Horel, John D., and X. Dong 2010: An evaluation of the distribution of Remote Automated Weather Stations (RAWS). *Journal of Appl. Meteor. and Clim.*, 49, 1563-1578.
- Jimenez, D, Forthofer, JM, Reardon, JJ, Butler, BW (2007) Fire Behavior sensor package remote trigger design. In 'The Fire Environment-innovations, management, and policy. Destin, FL', 26-30 March, 2007. (Eds BW Butler, W Cook) Volume RMRS-P-46CD pp. 662. (US Dept. of Agriculture, Forest Service, Rocky Mountain Research Station
- McCaffrey, BJ, Heskestad, G (1976) A robust bidirectional low-velocity probe for flame and fire application. *COMBUSTION AND FLAME* 26, 125-127.
- Morandini, F, Silvani, X (2010) Experimental investigation of the physical mechanisms governing the spread of wildfires. *International Journal of Wildland Fire* 19, 570-582.
- Potter BE (2012) Atmospheric interactions with wildland fire behaviour – I. Basic surface interactions, vertical profiles and synoptic structures. *International Journal of Wildland Fire* 21(7) 779-801 <http://dx.doi.org/10.1071/WF11128>
- Rothermel RC (1972) 'A Mathematical model for predicting fire spread in wildland fuels.' USDA Forest Service, Intermountain Forest and Range Experiment Station Research Paper INT-115 (Ogden, UT)

- Rothermel, R. C. 1991. Predicting behaviour and size of crown fires in the Northern Rocky Mountains. Research Paper INT-438. Ogden, UT: U. S. Department of Agriculture, Forest Service, Intermountain Research Station. (23,585 KB; 46 pages).
- Van Wagner, C.E. Development and structure of the Canadian Forest Fire Weather Index System. 1987. Van Wagner, C.E. Canadian Forestry Service, Headquarters, Ottawa. Forestry Technical Report 35. 35 p.